Spatial Kernel Discriminant Analysis: Applied for Hyperspectral Image Classification

Soumia Boumeddane[1], Leila Hamdad[1], Sophie Dabo-Niang[2] and Hamid Haddadou[1]
[1]*Laboratoire de la Communication dans les Systèmes Informatiques, Ecole nationale Supérieure d'Informatique, BP 68M, 16309, Oued-Smar, Algiers, Algeria*
[2]*Laboratoire LEM, Université Lille 3, Lille, France*

Keywords: Kernel Density Estimation, Kernel Discriminant Analysis, Spatial Information, Supervised Classification.

Abstract: Classical data mining models relying upon the assumption that observations are independent, are not suitable for spatial data, since they fail to capture the spatial autocorrelation. In this paper, we propose a new supervised classification algorithm which takes into account the spatial dependency of data, named Spatial Kernel Discriminant Analysis (SKDA). We present a non-parametric classifier based on a kernel estimate of the spatial probability density function which combines two kernels: one controls the observed values while the other controls the spatial locations of observations. We applied our algorithm for hyperspectral image (HSI) classification, a challenging task due to the high dimensionality of data and the limited number of training samples. Using our algorithm, the spatial and spectral information of each pixel are jointly used to achieve the classification. To evaluate the efficiency of the proposed method, experiments on real remotely sensed images are conducted, and show that our method is competitive and achieves higher classification accuracy compared to other contextual classification methods.

1 INTRODUCTION

Most statistical and machine learning methods assume that data samples are independent and identically distributed (i.i.d.). This assumed pre-condition about the independence of observations is not verified when dealing with spatial data (Cheng et al., 2014a) captured in many fields such as ecology, image analysis, epidemiology and environmental science. In fact, spatial data are characterized by spatial autocorrelation or spatial dependency phenomenon. This characteristic is defined as the tendency of near observations to be more similar than distant observations in space (Cheng et al., 2014b). This property is formulated as the first law of geography : "Everything is related to everything else, but near things are more related than distant things" (Tobler, 1970). For example, measurements taken in neighboring sites are more likely to be similar then those of distant locations, natural phenomena vary gradually over space and objects of similar characteristics tend to be clustered (ex: population with similar socio-economic characteristics and preferences,...etc) (Shekhar et al., 2009).

Ignoring this property of autocorrelation when analyzing spatial data may lead to inaccurate or inconsistent models or hypotheses (Shekhar et al., 2015), produce biased discriminant rules (Bel et al., 2009), hide important insight and could even invert patterns (Stojanova et al., 2013). An effective analysis of spatial data must take into account geographic positions of observations and the existing relationship due to their proximity.

Several supervised learning methods modeling spatial dependency for classification and regression are considered in the literature: Markov Random Field-based Bayesian classifiers, which integrates the spatial information of data via the a priori term in Bayes rule ; The logistic spatial autoregression (SAR) model, which models the spatial dependence directly in the regression equation using a neighborhood relationship contiguity matrix and a weight of the spatial dependency; and Geographically Weighted Regression (GWR) which includes a spatial variation parameter in regression equation (Shekhar et al., 2011). More recently, (Stojanova et al., 2013) proposed SCLUS (Spatial Predictive Clustering System), a predictive clustering tree framework that learn from spatial autocorrelated data .

Various indices are proposed to measure the spatial autocorrelation, from a global or a local point of

Boumeddane, S., Hamdad, L., Dabo-Niang, S. and Haddadou, H.
Spatial Kernel Discriminant Analysis: Applied for Hyperspectral Image Classification.
DOI: 10.5220/0007372401840191
In *Proceedings of the 11th International Conference on Agents and Artificial Intelligence (ICAART 2019)*, pages 184-191
ISBN: 978-989-758-350-6

view, such as : Moran's I index, c index of Geary, Cliff and Ord indices, Getis and Ord (G_i et G_i^*) indices and Local Indicators of Spatial Association (LISA) (Shekhar et al., 2015).

We focus in this work on supervised classification task. We propose a new classification algorithm for spatially autocorrelated data, that we call SKDA, for Spatial Kernel Discriminant Analysis. Our algorithm is a spatial extension of classical Kernel Discriminant Analysis rule; it is founded on a kernel estimate of the spatial probability density function that integrates two kernels: one controls the observed values while the other controls the spatial locations of observations (Dabo-Niang et al., 2014).

One potential application of our SKDA algorithm is the classification of remotely sensed hyperspectral images. This problem has attracted a lot of attention over the past decade. Several studies proposed spectral-spatial classification algorithms which integrate spatial context and spectral information of the hyperspectral image. This incorporation of spatial information has shown great impact for improving classification accuracy (He et al., 2017). According to the way the spatial dimension is incorporated, these methods can be classified into three main categories: integrated spectral-spatial approaches, preprocessing-based approaches, and post-processing-based approaches (Fauvel et al., 2013). A survey about the incorporation of spatial information for HSI classification is presented in (Wang et al., 2016).

The contribution of our work is double; on one hand, we propose a spatial classification algorithm managing the dependency of data, on the other hand, a spatial-spectral method is proposed for the classification of HSI with competitive results.

The remainder of the paper is organized as follows: Section 2 defines the context of this study, and presents the background knowledge essential to the understanding of our algorithm. Section 3 presents our SKDA algorithm. Section 4 shows experimental results of our method on hyperspectral image classification. Finally, section 5 summarizes the results of this work and draws conclusions.

2 BACKGROUND

In this section, we begin by formally defining the necessary notations that we will adopt throughout this paper. Then, present the background knowledge essential to the understanding of our algorithm.

In this work, we focus on geostatistical data, we consider a spatial process $\{Z_i = (X_i, Y_i) \in \mathbb{R}^d \times \mathbb{N}, i \in \mathbb{Z}^N, d \geq 1, N \in \mathbb{N}^*\}$, defined over a probability space (Ω, F, P) and indexed in a rectangular region $I_n = \{i \in \mathbb{Z}^N : N \in \mathbb{N}^*, 1 \leq i_k \leq n_k, \forall k \in \{1,...,N\}\}$. Where a point $i = (i_1,...,i_N) \in \mathbb{Z}^N$ is called a site, representing a geographic position. And let $\hat{n} = n_1 \times n_2 \times ... \times n_N = Card(I_n)$ be the sample size, and f(.) the density function of $X \in \mathbb{R}^d$. Each site $i \in I_n$ is characterized by a d-dimensional observation $x_i = (x_{i1}, x_{i2}, ..., x_{id})$.

In this work we are interested on supervised classification which consists of building a classifier that from a given training set containing input-output pairs allows to predict a class $Y_i \in \{1,2,...,m\}$ of a new observation x_i .

2.1 Bayes Classifier

Bayes classifier is one of the widely used classification algorithms due to its simplicity, efficiency and efficacy. It is a probabilistic classifier which rely on Bayes' theorem and the assumption of independence between the features, in other words, the classification decision is made basing on probabilities. It consist of assigning an instance x to the class with the highest a posteriori probability.

Supposing that we have m classes, associated each with a probability density function f_k where $f_k = P(x/k)$ and an a priori probability π_k that an observation belongs to the class k, $k \in \{1,2,...,m\}$. Bayes discriminant rule is formulated as follows :

$$Assign\ x\ to\ class\ k_0\ where\ k_0 = arg^{max}_{k\in\{1,2,...,m\}}(\pi_k f_k(x)) \quad (1)$$

2.2 Kernel Density Estimation

As we might notice, Bayesian methods require a background knowledge of many probabilities, which consists of a practical difficulty to apply it. To avoid these requirements, these probabilities can be estimated based on available labeled data or by making assumptions about the distributions (Gramacki, 2018). Two classes of density estimators are recognized in the literature. The first, known as parametric methods are based upon the assumption that data are drawn form an arbitrary well known distribution (e.g. Gaussian, Gamma, Cauchy ... etc.) and finding the best parameters describing this distribution . Two commonly used techniques can be sited: Bayesian parameter estimation and maximum likelihood. However, this assumption about the form of the underlying density is not always possible because of the complexity of data. In such cases, nonparametric estimation techniques are required. These methods do not make any a priori assumptions about the distri-

bution but estimate the density function directly from the data (Gramacki, 2018).

One of the most known non-parametric density estimation techniques is Kernel Density Estimation (KDE). First contributions concerning kernel estimation of (Parzen, 1962) and (Rosenblatt, 1985) for spatial densities are due to (Tran, 1990). A marginal density of a point $x \in \mathbb{R}^d$ is defined as :

$$\hat{f}(x) = \frac{1}{\hat{n}h^d} \sum_{i \in I_n} K\left(\frac{x - X_i}{h}\right), x \in \mathbb{R}^d \qquad (2)$$

Where h is a smoothing parameter called bandwidth and K is a weight function, called "kernel" which decreases as the distance between x and X_i increases. This function satisfies the following condition:

$$\int_{-\infty}^{+\infty} K(x)\,\mathrm{d}x = 1 \qquad (3)$$

Different kernel functions have been proposed in the literature: Uniform, Triangle, Epanechnikov ... etc.

KDE is a relevant tool for analyzing and visualizing the distribution of spatial process. Moreover, it is one of the most common methods for hotspots mapping, used for crash and crimes data (Chainey et al., 2008).

2.3 Kernel Discriminant Analysis

Replacing class densities f_i in Bayes discriminant rule (Equation 1) by its kernel density estimate given in Equation 2 , define a new classifier known as Kernel Discriminant Rule , the base of Kernel Discriminant Analysis supervised algorithm. According to Kernel Discriminant Rule, an observation $x \in \mathbb{R}^d$ will be assigned to the group k_0 which maximize $\hat{\pi}_k \hat{f}_k(x)$. Where $\hat{\pi}_k$ is an estimator of the a priori probabilities π_k , given by

$$\hat{\pi}_k = \frac{m_k}{\hat{n}} \qquad (4)$$

and m_k is the size of the k-th class.

2.4 Spatial KDE

Kernel density estimator previously presented does not take into account spatial autocorrelated data. In fact, to estimate a density at a site, all the data points are used and no specific weight is given to neighboring sites. In (Dabo-Niang et al., 2014), the authors proposed a kernel density estimation of a spatial density function, which incorporates spatial dependency of data. They propose a new version of (Tran, 1990) estimator (Equation 2) which has the particularity of taking into account not only the values of the observations but also the position of sites where the observations occurred. They established its uniform almost sure convergence and they studied the consistency of its mode. They proposed a spatial density estimation of a discretely indexed spatial process i.e. a random field $(X_i, i \in \mathbb{Z}^N, N > 1)$, with values in $\mathbb{R}^d, d \geq 1$ and defined over a probability space (Ω, F, P).

For each observation $x_j \in \mathbb{R}^d$ located at a site $j \in I_n$, this spatial density estimator is defined as follows:

$$\hat{f}(x_j) = \frac{1}{\hat{n}h_v^d h_s^N} \sum_{i \in I_n} K_1\left(\frac{x_j - X_i}{h_v}\right) K_2\left(\frac{\|i-j\|}{h_s}\right) \qquad (5)$$

Where

- h_v and h_s are two bandwidths controling observations (values) and sites position respectively,
- K_1 and K_2 are two kernels respectively defined in $\mathbb{R}^d$ and $\mathbb{R}$, where the first manage observation values while the second deals with spatial locations of these observations.
- And $\| i - j \|$ is the euclidean distance between sites i and j .

In the case where I_n is a rectangular grid i.e. $N = 2$, Equation 5 become;

$$\hat{f}(x_j) = \frac{1}{\hat{n}h_v^d h_s^2} \sum_{i \in I_n} K_1\left(\frac{x_j - X_i}{h_v}\right) K_2\left(\frac{\|i-j\|}{h_s}\right) \qquad (6)$$

The incorporation of a second kernel K_2 allows this estimator to give a weight to sites, which decrease as the distance between corresponding sites increases. Consequently, to estimate $f(x_j)$ at a site j, only the neighboring sites are considered because they can bring sufficient information about the distribution of X_j , which means that the farther a site i is from j, the lower is the dependence between X_i and X_j. More details about this estimator can be found in (Dabo-Niang et al., 2014).

3 SPATIAL KERNEL DISCRIMINANT ANALYSIS

In what follows, we propose a novel supervised spatial classification algorithm allowing a classification of an observation at a new site, based not only on the observation itself but taking in consideration the position of sites. In other words, the classification is based on the observations of neighboring sites. The totality of data is exploited to achieve the classification: the value of the observation, the position of the new site and training model from the nearby sites.

We present a new kernel discriminant rule for strongly mixing random fields, which means that sites located at a proximity are more dependent than distant sites. Thus, if a distance between two sites is high, their values are independent and it is more likely that they belongs to different classes.

Our classification rule consists of assigning a new observation $x \in \mathbb{R}^d$ at a site i_0 to the class k_0 where $k_0 = arg^{max}_{k\in\{1,2,...,m\}}(\hat{\pi}_k \hat{f}_k(x))$

Where $\hat{\pi}_k$ is estimated as follow:

$$\hat{\pi}_k = \frac{m_k}{\hat{N}} \tag{7}$$

Suppose that $X_{k1}, X_{k2}, ..., X_{kmk}$ are d-dimensional observations from the k-th class, spatial Kernel Density estimate is defined as follows (based on (Dabo-Niang et al., 2014) estimator):

$$\hat{f}_k(x_j) = \frac{1}{m_k h_v^d h_s^2} \sum_{\substack{i\in I_n,\\ C(X_{ki})=k}} K_1\left(\frac{x_j - X_{ki}}{h_v}\right) K_2\left(\frac{\|i-j\|}{h_s}\right) \tag{8}$$

Where

- C(.) is the class label of an observation,
- m_k is the size of k-th class in the training data
- $\hat{N}$ is the size of the training set

The kernel function K_1 is a multivariate kernel with values in $\mathbb{R}^d$. In this work, we suggest to define this kernel as a multiplicative kernel, as follows:

For $X = (x_1, x_2, ..., x_d)$ in $\mathbb{R}^d$:

$$K_1(X) = K(x_1) \times K(x_2) \times ... \times K(x_d) \tag{9}$$

Where: K is a univariate Kernel. More specifically:

$$K_1\left(\frac{x_j - X_i}{h_v}\right) = K\left(\frac{x_{j1} - X_{i1}}{h_v}\right) \times ... \times \left(\frac{x_{jd} - X_{id}}{h_v}\right) = \prod_{l=1}^{d} K\left(\frac{x_{jl} - X_{il}}{h_v}\right)$$

We summarize in Algorithm 1 the main steps of our SKDA technique. We precise that, in order to decrease the execution time of our algorithm, the term $K_1(.)$ in Equation 8 is computed only when the term $K_2(.) \neq 0$. In addition, for a testing set, step 2 in Algorithm 1, is executed one time.

Algorithm 1: Spatial Kernel Discriminant Analysis algorithm.

Result:
- Classfication of an observation at a new site

Input :
- X_{i0} : an observation to be classified, situated at a site i_0
- A set of training data $(X_i, y_i) \in \mathbb{R}^d \times \{1, 2, .., m\}$, where y_i is the class label of X_i

Output:
- k_0 : the class label of X_{i0}

1 **foreach** *class* $k \in \{1, 2, ..., m\}$ **do**
2 Compute a priori probability $\hat{\pi}_k$ (using Equation 7)
3 Compute $\hat{f}_k(x_{i0})$ using Equation 8, based on learning data of the k-th class
4 **end**
5 $k_0 = arg^{max}_{k\in\{1,2,...,m\}}(\hat{\pi}_k \hat{f}_k(x))$

4 EXPERIMENTAL RESULTS

4.1 Hyperspectral Images Classification

One potential application of our algorithm on real data would be the classification of remotely sensed hyperspectral images. A hyperspectral image (HSI) is a set of simultaneous images collected for the same area on the surface of the earth with hundreds of spectral bands at different wavelength channels and with high resolution (He et al., 2017). A HSI is represented as a hyperspectral cube with spectral and spatial dimension (Figure 1). Each pixel is described by its position and a spectral vector, where its size correspond to the number of spectral bands collected by the sensor (Fauvel et al., 2013).

Hyperspectral image classification consists of assigning a unique label to a pixel vector, representing a thematic class such as forest, urban, water, and agriculture. These images are considered as a relevant tool for many applications, such as ecology, geology, hydrology, precision agriculture, and military applications (Ghamisi et al., 2017).

Using our classification algorithm in this context is considered as spectral-spatial classification technique which exploits all information available in an HSI to achieve better accuracy of classification.

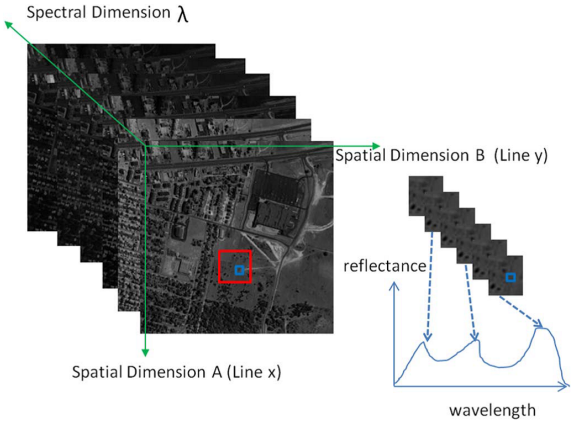

Figure 1: Hyperspectral image representation.

4.2 Data Set

In order to evaluate and validate the effectiveness of our method, we carried out experiments on a widely used real-world hyperspectral image dataset: the Indian Pines benchmark[1]. The scene represents Pine forests of Northwestern Indiana in America in 1992. This data set is a very challenging land-cover classification problem, due to the presence of mixed pixels (Appice et al., 2017) and the non-proportionality between the size of different classes. In addition, the crops (mainly corn and soybeans) of this scene are captured in early stages of growth with less than 5% coverage, which makes discrimination between these crops a difficult task.

This scene was captured using NASA's Airborne Visible/Infrared Imaging Spectrometer (AVIRIS) sensor, with a size of 145×145 pixels, classified into 16 ground-truth land-cover classes, where each class contains from 20 to 2468 pixels. The effective size of this dataset is 10249 pixels after removing the image background (pixels with a label equal to zero). Each pixel is characterized by 200 spectral bands, after eliminating 20 noisy channels corresponding to the water absorption bands. The color composite image and the corresponding ground truth map are shown in Figure 2.

Due to the expensive cost of manual labeling of hyperspectral images pixels, the number of training samples is often limited, this represent a challenging task for classification algorithms (Ghamisi et al., 2017). Thus, our SKDA algorithm should be capable to well-perform even if only a few labelled samples are available. To build the training set, we randomly selected only 10% of pixels from each class, and the remaining pixels forms the test set.

[1]Available on www.ehu.eus/ccwintco/index.php/Hyperspectral_Remote_Sensing_Scenes

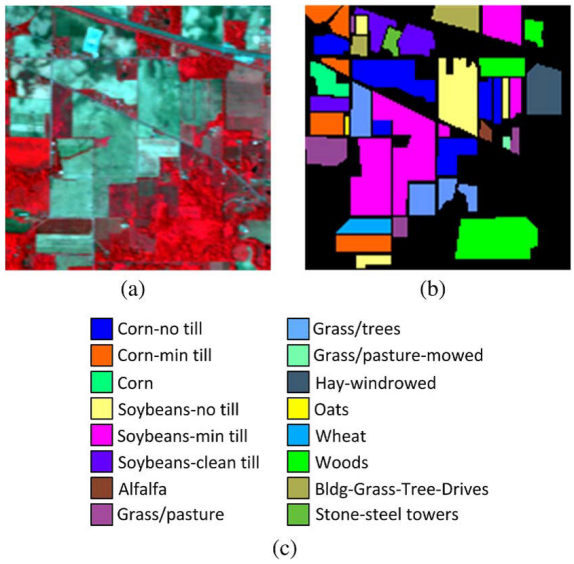

Figure 2: Indian Pines image. (a) Three-band color composite. (b) Reference data. (c) Color code.

Table 1: Class labels and the number of training and testing samples for Indian pines.

-	Class	Train	Test	Total
1	Alfalfa	4	42	46
2	Corn-no till	142	1286	1428
3	Corn-min till	83	747	830
4	Corn	23	214	237
5	Grass-pasture	48	435	483
6	Grass-trees	73	657	730
7	Grass-pasture-mowed	2	26	28
8	Hay-windrowed	47	431	478
9	Oats	2	18	20
10	Soybean-no till	97	875	972
11	Soybean-min till	245	2210	2455
12	Soybean-clean	59	534	593
13	Wheat	20	185	205
14	Woods	126	1139	1265
15	Build-Grass-Trees-Drives	38	348	386
16	Stone-Steel-Towers	9	84	93
	Total	1018	9231	10249

Table 1 shows the size of training and testing sets of each class of Indian Pines scene.

4.3 Performance Comparison

To evaluate the performance of our algorithm compared to other methods, we employ three widely used classification accuracy measures: Overall accuracy (OA), Average Accuracy (AA) and per class accuracy.

OA is defined as the ratio between the number of well-classified pixels to the size of testing set, while AA is the average of per-class classification accuracies.

The results of classification depends on the training and testing sets which are randomly selected. To reduce this effect and make the comparison fair, we repeat each experiment 10 times with different training and testing sets and we report the mean accuracy of these executions. We use Epanechnikov Kernel for the two kernels K_1 and K_2 with observation bandwidth h_v equal to 700 and a spatial bandwidth h_s of 3. We obtained these optimal values of h_v and h_s bandwidths by studying their influence on overall and average classification accuracies. In fact, we varied empirically the values of these two bandwidth, and select the combination which gave the highest OA and AA.

In this section, we present the quantitative results achieved by our SKDA algorithm and the results of nine different methods reported from (Zhou et al., 2018). To have a fair comparison we use the same ratio of training and testing set as this work. Tables 2 shows the classification accuracy for each class, overall accuracy (OA) and average accuracy (AA), where the best accuracies are in bold.

Table 2 demonstrates that our proposed SKDA algorithm outperforms other methods, with an improvement of Average Accuracy by 5,58%, the Overall Accuracy by 3,04% and per-class accuracy till 16,11% (expect for Wheat class) comparing to SSLSTMs approach.

It can be observed that spectral-spatial approaches (MDA, CNN, LSTM-based methods and SKDA) gives significantly better accuracies then pixel-wised methods (PCA, LDA, NWFE, RLDE) which are based only on observations values.

Figure 3 visualize the classification result of Indian pines data set using our SKDA algorithm and the training data used for density estimation.

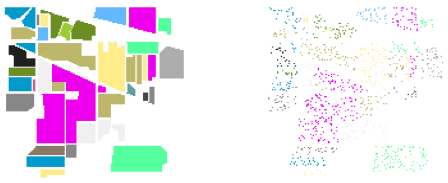

(a) Indian Pines dataset (b) Training set

(c) SKDA classification result, $h_v = 700$, $h_s = 3$

Figure 3: Classification visualisation.

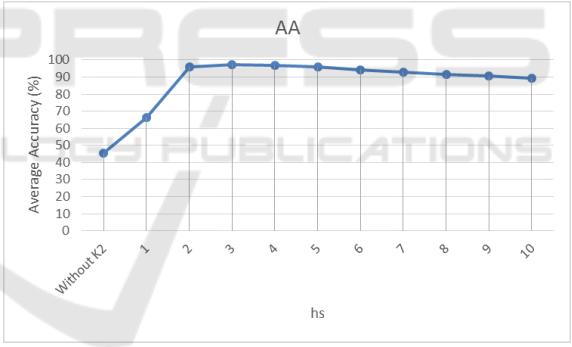

(a) The effect of hs bandwidth on AA.

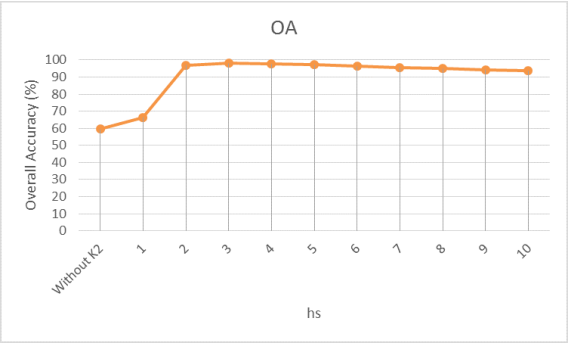

(b) The effect of hs bandwidth on OA.

Figure 4: Influence of spatial bandwidth.

4.4 Influence of Parameters

Our classification algorithm depends on two bandwidths: h_v and h_s, that control observation values and spatial neighborhood respectively. In this section, we analyze the impact of the integration of the spatial dimension of data in the classification process through the study of the influence of the spatial bandwidth h_s on overall and average accuracies. We set the value of the bandwidth h_v to 700, and we vary h_s from 1 to 10 and compare the results also with classical version of Kernel Discriminant Analysis that don't take into account the spatial context of data (the estimation of density is based only on the values of observations i.e the second kernel K_2 is not used).

Table 2: Classification accurracy (%) for Indian Pines data set.

Label	PCA	LDA	NWFE	RLDE	MDA	CNN	SeLSTM	SaLSTM	SSLSTMs	**SKDA**
OA	72.58	76.67	78.47	80.97	92.31	90.14	72.22	91.72	95.00	**98.04**
AA	70.19	72.88	76.08	80.94	89.54	85.66	61.72	83.51	91.69	**97.27**
1	59.57	63.04	62.17	64.78	73.17	71.22	25.85	85.85	88.78	**98.57**
2	68.75	72.04	76.27	78.39	93.48	90.10	66.60	89.56	93.76	**96.88**
3	53.95	57.54	59.64	68.10	84.02	91.03	54.83	91.43	92.42	**96.59**
4	55.19	46.58	59.83	70.80	83.57	85.73	43.94	90.61	86.38	**96.77**
5	83.85	91.76	88.49	92.17	96.69	83.36	83.45	88.60	89.79	**96.78**
6	91.23	94.41	96.19	94.90	99.15	91.99	87.76	90.81	97.41	**99.75**
7	82.86	72.14	82.14	85.71	93.60	85.60	23.20	51.20	84.80	**95.38**
8	93.97	98.74	99.04	99.12	99.91	97.35	95.40	99.02	99.91	**99.97**
9	34.00	26.00	44.00	73.00	63.33	54.45	30.00	38.89	74.44	**90.55**
10	64.18	60.91	69.18	69.73	82.15	75.38	71.29	88.64	95.95	**96.73**
11	74.96	76.45	77.78	79.38	92.76	94.36	75.08	94.62	96.93	**98.74**
12	41.72	67.45	64.05	72.28	91.35	78.73	54.49	86.10	89.18	**96.10**
13	93.46	96.00	97.56	97.56	**99.13**	95.98	91.85	90.11	98.48	99.02
14	89.45	93.79	93.49	92.36	98.22	96.80	90.37	98.10	98.08	**99.92**
15	47.77	65.54	58.50	67.10	87.84	96.54	30.49	88.59	92.85	**98.33**
16	88.17	83.66	89.03	89.68	94.29	81.90	62.86	64.05	87.86	**96.30**

Figure 4 shows overall and average accuracies as a function of h_s bandwidth. This plot proves that the integration of the spatial dimension of data improves drastically the classification accuracy, and that the results obtained by our SKDA algorithm exceeds those obtained by classical KDA. In fact, the AA increased from 45% to 70% when spatial dependency is considered (when $h_s = 1$). Best accuracies were obtained when $h_s = 3$, with an Average Accuracy of 97,27% and an Overall Accuracy of 98,04% (as mentioned in the previous section). However, when greater values of h_s are used, a degradation of OA and AA is captured.

This experiment proves that the choice of the spatial bandwidth h_s is crucial. In fact, small values of this bandwidth are not sufficient for the learning model; while, larger values decrease the classification accuracy because they lead to an over-smoothing of the density.

5 CONCLUSION

In this paper, a Kernel Discriminant Analysis algorithm for spatial data named SKDA is proposed. This supervised classification algorithm allows taking into consideration the spatial autocorrelation of data, and exploiting all the available information: the observations in one hand and their positions in other hand. Another contribution of this work is the proposition of a new spatial-spectral hyperspectral image classification algorithm. Experimental tests on real word dataset shows that our SKDA algorithm outperforms other contextual classification algorithms and proves that the integration of the spatial dimension of data increases the classification accuracy, even with limited number of training samples and high-dimensionality of data. Experiments on other hyperspectral images benchmark datasets are ongoing. Moreover, we aim to propose an efficient way for bandwidths tuning, since the classification accuracy depends on.

REFERENCES

Appice, A., Guccione, P., and Malerba, D. (2017). A novel spectral-spatial co-training algorithm for the transductive classification of hyperspectral imagery data. *Pattern Recognition*, 63:229–245.

Bel, L., Allard, D., Laurent, J. M., Cheddadi, R., and Bar-Hen, A. (2009). CART algorithm for spatial data: Application to environmental and ecological data. *Computational Statistics & Data Analysis*, 53(8):3082–3093.

Chainey, S., Tompson, L., and Uhlig, S. (2008). The utility of hotspot mapping for predicting spatial patterns of crime. *Security journal*, 21(1-2):4–28.

Cheng, T., Haworth, J., Anbaroglu, B., Tanaksaranond, G., and Wang, J. (2014a). Spatiotemporal data mining. In *Handbook of regional science*, pages 1173–1193. Springer.

Cheng, T., Wang, J., Haworth, J., Heydecker, B., and Chow, A. (2014b). A dynamic spatial weight matrix and localized space–time autoregressive integrated moving average for network modeling. *Geographical Analysis*, 46(1):75–97.

Dabo-Niang, S., Hamdad, L., Ternynck, C., and Yao, A.-F. (2014). A kernel spatial density estimation allowing for the analysis of spatial clustering. application

to monsoon asia drought atlas data. *Stochastic environmental research and risk assessment*, 28(8):2075–2099.

Fauvel, M., Tarabalka, Y., Benediktsson, J. A., Chanussot, J., and Tilton, J. C. (2013). Advances in spectral-spatial classification of hyperspectral images. *Proceedings of the IEEE*, 101(3):652–675.

Ghamisi, P., Plaza, J., Chen, Y., Li, J., and Plaza, A. J. (2017). Advanced spectral classifiers for hyperspectral images: A review. *IEEE Geoscience and Remote Sensing Magazine*, 5(1):8–32.

Gramacki, A. (2018). *Nonparametric Kernel Density Estimation and Its Computational Aspects*. Springer.

He, L., Li, J., Plaza, A., and Li, Y. (2017). Discriminative low-rank gabor filtering for spectral-spatial hyperspectral image classification. *IEEE Trans. Geoscience and Remote Sensing*, 55(3):1381–1395.

Parzen, E. (1962). On estimation of a probability density function and mode. *The annals of mathematical statistics*, 33(3):1065–1076.

Rosenblatt, M. (1985). Stationary sequences and random fields.

Shekhar, S., Evans, M. R., Kang, J. M., and Mohan, P. (2011). Identifying patterns in spatial information: A survey of methods. *Wiley Interdisc. Rew.: Data Mining and Knowledge Discovery*, 1(3):193–214.

Shekhar, S., Jiang, Z., Ali, R. Y., Eftelioglu, E., Tang, X., Gunturi, V. M. V., and Zhou, X. (2015). Spatiotemporal data mining: A computational perspective. *ISPRS Int. J. Geo-Information*, 4(4):2306–2338.

Shekhar, S., Kang, J., and Gandhi, V. (2009). Spatial data mining. In *Encyclopedia of Database Systems*, pages 2695–2698. Springer.

Stojanova, D., Ceci, M., Appice, A., Malerba, D., and Dzeroski, S. (2013). Dealing with spatial autocorrelation when learning predictive clustering trees. *Ecological Informatics*, 13:22–39.

Tobler, W. R. (1970). A computer movie simulating urban growth in the detroit region. *Economic geography*, 46(sup1):234–240.

Tran, L. T. (1990). Kernel density estimation on random fields. *Journal of Multivariate Analysis*, 34(1):37–53.

Wang, L., Shi, C., Diao, C., Ji, W., and Yin, D. (2016). A survey of methods incorporating spatial information in image classification and spectral unmixing. *International Journal of Remote Sensing*, 37(16):3870–3910.

Zhou, F., Hang, R., Liu, Q., and Yuan, X. (2018). Hyperspectral image classification using spectral-spatial lstms. *Neurocomputing*.